ORIGINAL ARTICLE

Biomechanical analysis and design of a dynamic spinal fixator using topology optimization: a finite element analysis

Hung-Ming Lin · Chien-Lin Liu · Yung-Ning Pan · Chang-Hung Huang · Shih-Liang Shih · Shun-Hwa Wei · Chen-Sheng Chen

Abstract Surgeons often use spinal fixators to manage spinal instability. Dynesys (DY) is a type of dynamic fixator that is designed to restore spinal stability and to provide flexibility. The aim of this study was to design a new spinal fixator using topology optimization [the topology design (TD) system]. Here, we constructed finite element (FE) models of degenerative disc disease, DY, and the TD system. A hybrid-controlled analysis was applied to each of the three FE models. The rod structure of the topology optimization was modelled at a 39 % reduced volume compared with the rigid rod. The TD system was similar to the DY system in terms of stiffness. In contrast, the TD system reduced the cranial adjacent disc stress and facet contact force at the adjacent level. The TD system also reduced pedicle screw stresses in flexion, extension, and lateral bending.

1 Introduction

Spinal surgeries, including traditional and minimally invasive deformity correction, are often used to manage spinal instability [1]. In contrast to the traditional open approach, minimally invasive spinal surgery presents several advantages. For example, minimally invasive deformity corrections are associated with relatively short operating times, reduced medical complications, smaller incisions, no muscle stripping, less anaesthesia, shorter hospital stays, quicker recuperation periods, and reduced blood loss. However, minimally invasive deformity corrections must be technically feasible to be readily duplicated and widely adapted [2]. Additionally, with respect to surgical implants, spinal fusion surgery is the traditional procedure, and it has clinically curative effects [2]. However, spinal fusion surgeries have other problems, including donor ailments, inherent surgery-associated morbidity rates, and adjacent segment disease [1, 3, 4]. Several clinical reports have demonstrated that spinal fusion surgery may accelerate degeneration at adjacent segments [5, 6]. Consequently, several flexible posterior spinal fixation systems have gradually been introduced into the clinic [1, 7, 8]. These implants are designed to restore spinal stability and reduce the load on the adjacent disc. The Dynesys (DY) system (Zimmer, Minneapolis, MN, USA) is a type of dynamic stabilization device that has been used in clinics for more than a decade. The DY system consists of polycarbonate urethane (PCU) spacers, polyethylene terephthalate (PET) cords, and titanium alloy pedicle screws.

H.-M. Lin · Y.-N. Pan
Department of Mechanical Engineering, National Taiwan University, Taipei, Taiwan

C.-L. Liu
Department of Orthopedic Surgery, Taipei Veterans General Hospital, Taipei, Taiwan

C.-H. Huang
Department of Medical Research, Mackay Memorial Hospital, Tamshui District, New Taipei City, Taiwan

S.-L. Shih
Department of Orthopaedic Surgery, Zhong-Xing Branch of Taipei-City Hospital, Taipei, Taiwan

S.-H. Wei · C.-S. Chen (✉)
Department of Physical Therapy and Assistive Technology, National Yang-Ming University, 155, Sec. 2, Li-Nung St., Taipei 112, Taiwan
e-mail: cschen@ym.edu.tw

The length of the PCU spacers can be adapted for the clinical situation, the PET cords are introduced through the screw heads, and the PCU spacers are interposed and fixed after pre-loading [8, 9]. Moreover, a previous clinical study [10] indicated that the DY system produced satisfactory outcomes, with the patient satisfaction reported to be as high as 95 %. However, complications, including slight screw loosening (3 of 26 patients), adjacent segment degeneration (47 % patients), and screw breakage with low back pain (one patient), were observed at a 4-year follow-up. Various clinical studies [10–12] have addressed the similarity in stiffness between the DY system and a rigid fixation system. Previous clinical literature [10–12] has also addressed that the incidence of adjacent level degeneration in patients using the DY system was similar to that observed in patients using a rigid fixation system. Biomechanically, the DY system reduces the range of motion (ROM) of the intact spine [13–16], but the DY system is more flexible than a rigid internal fixator [17]. Additionally, previous biomechanical investigations have demonstrated that the DY system provides greater stiffness [17, 18]. Niosi et al. [15, 19] indicated that a DY system with long spacers typically results in increased ROM and a decrease in facet loads compared to a system with shorter spacers.

Conversely, Chen et al. [20] sought to devise a new intervertebral cage design to allow more bone graft volume using topology optimization. They obtained a new cage that had a volume of 1,603 mm^3, which was significantly smaller than the initial cage model (2,058 mm^3). The new design provided satisfactory ROM and stress levels at the adjacent disc, but it displayed a higher stress level than the original cages. Lin et al. [21] demonstrated the ability to use the optimized topology design (TD) in lumbar fusion cages made from Ti-6Al-4V alloy using a rapid prototyping process, i.e. selective laser melting (SLM) (Fraunhofer ILT, Aachen, Germany), to achieve the designed spatial arrangement of material and to reproduce the designed microstructure features. Topology optimization algorithms [21–23] generate an optimized material distribution for a set of loads and constraints within a given design space. Radiographic characterizations and mechanical properties were investigated to determine how the structural characteristics of the fabricated cage were reproduced from design characteristics using micro-computed tomography scanning. The new, porous Ti-6Al-4V optimal-structure cage displayed consistent mechanical properties; thus, it can be a promising alternative for use as a porous implant for spine fusion. Furthermore, Goel et al. [1] indicated the importance of optimizing the dynamic implant stiffness to achieve the desired spinal ROM.

Hence, the aim of this study was to design a new spinal fixator using topology optimization [20–26] (TD system; TD system) to reduce the overall stiffness and volume. The lumbar spine with the TD system was evaluated in terms of ROM, disc stress, facet joint force, and pedicle screw stress.

2 Materials and methods

2.1 Validation of the FE model

A three-dimensional, nonlinear finite element (FE) model of the human lumbar spine was created using the commercial software, ANSYS 11.0 (ANSYS Inc., Canonsburg, PA, USA), as described in our previous studies [27–30]. A detailed description of this lumbar spine FE model was previously reported [27–30]. Previous studies [27–30] have indicated that an FE intact model of the L1–L5 lumbar spine was created using computed tomography scanned files. To obtain reliable data, the convergence test and model were validated [28, 29]. For the convergence test [28, 29], three mesh densities (4,750 elements/4,960 nodes, coarse mesh density model; 27,244 elements/30,630 nodes, normal mesh density model; and 84,594 elements/94,162 nodes, finest mesh density model) were chosen to test for any ROM changes occurring in the intact model, and the finest mesh density was selected because the change was within 1.03 % (<0.2°). For model validation [28, 29], the ROM in the five levels of the intact model was validated using previous cadaveric in vitro tests. The FE intact model displayed stiffer behaviour in flexion, with an ROM value that was 4° less than that described in Rohlmann's in vitro study. In addition, softer results were obtained in extension and torsion compared with the in vitro test data; however, the differences were still within 2°. Overall, the discrepancy between the in vitro tests and our FE simulation was within one standard deviation.

Although our FE model was developed in a previous study [20], it did not consider degenerated discs. Therefore, this study varied the material properties of degenerated discs and evaluated the ROM and annulus stress of a degenerated lumbar spine. Umehara et al. [31] reported that the Young's modulus of the ground substance of the annulus increased as the disc degenerated. Thus, the corresponding Young's modulus (E) of the degenerated discs in each test increased by 10 % relative to the intact disc. This FE model extracted the L4–L5 motion segment from the entire lumbar spine model to test the degenerated disc. The degenerated disc was simulated with hyperelasticity behaviour, and the material properties were controlled

using two parameters (C1 and C2) in the Mooney–Rivlin formulation. The degenerated L4–L5 model was validated experimentally [32] by measuring the ROM using a 7.5-Nm moment for flexion–extension, lateral bending, and torsion. The experimental results [32] indicated that the grading system of intervertebral disc degeneration agreed with the system of Wilke et al. [33]; each of these parameters was classified on a scale ranging from 0 (no degeneration) to 3 (severe degeneration). Grade II disc degeneration represented moderate degeneration. To examine any discrepancies, the FE analysis was compared with a previous in vitro test [32] using the following equation:

degeneration. However, the DDD model, which consisted of 112,174 elements and 94,162 nodes, did not include the spinal fixation system.

2.2 New design of dynamic spinal fixator using topology optimization

In the clinic, several reports have demonstrated that spinal fusion surgery accelerated degeneration at adjacent segments due to the higher stiffness from the rigid rod [5, 6]. Some spinal implants, such as the dynamic spinal fixator, have been substituted to reduce the stiffness of the spinal fixator while preserving the spinal ROM [34]. Conse-

$$error = \sqrt{(ROM_P - ROM_E)^2_{flexion + extension} + (ROM_P - ROM_E)^2_{lateralbending} + (ROM_P - ROM_E)^2_{torsion}}$$

ROM_P: the ROM in the present FE study, ROM_E: the ROM in the previous in vitro test.

The FE analysis exhibited a similar trend to that observed in previous experimental results (Fig. 1). When the Young's modulus of the annulus fibrosis of the disc was increased by 100 % (the corresponding Young's modulus (E) was 6.3 MPa), the ROM of L4–L5 was closer to that of the in vitro results. The smallest error (0.72) was observed after applying a data normalization method.

Then, an entire lumbar spine model with degenerative disc disease (DDD) was created to compare the DY and TD models using the above parameters (disc annulus fibrosis: C1 = 0.84, C2 = 0.21; Young's modulus E = 6.3 MPa; nucleus: elastic modulus = 1.66 MPa; and Poisson's ratio = 0.499) to simulate the stabilization of grade II disc

quently, this study focuses on the distribution of global structural stiffness from the rod. For this purpose, we employed topology optimization to determine the redundant rod region that transmits the least strain energy. This study applied topological optimization software (ANSYS 11.0; ANSYS Inc., Canonsburg, PA) to design a new rod aimed at effectively reducing the stiffness of the rod.

The theory of topological optimization seeks to minimize the energy of structural compliance, termed the objective function. Minimizing compliance is equivalent to maximizing the global structural stiffness [20], so the standard formulation of topology optimization defines the problem as minimizing the structural compliance while satisfying a constraint on the volume (V) of the structure. The optimization problem is as follows:

Fig. 1 Validation of the error data and ROM
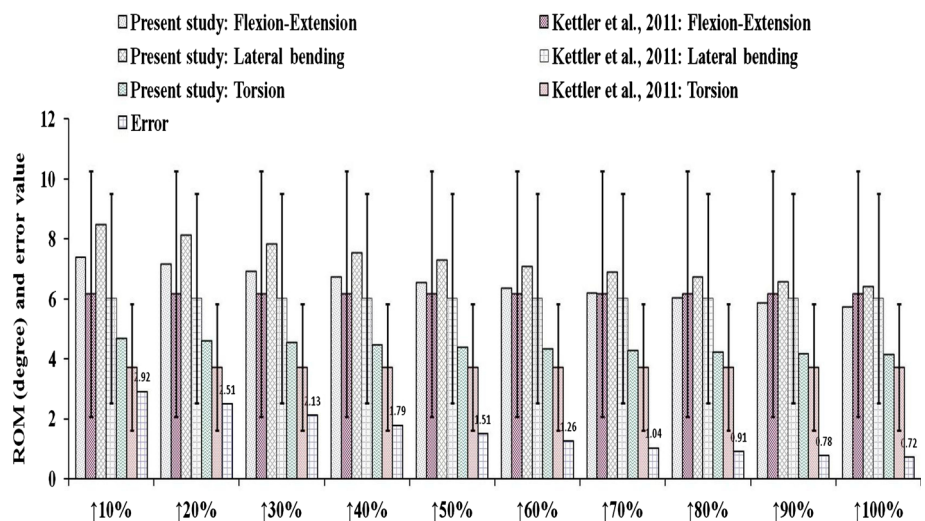
objective function : minimize (U_c)

limitation : $0 < \eta_i < 1 (i = 1, 2, 3, \ldots, n)$

$$V \le V_o - V^*$$

$$V = \sum_i^n \eta_i V_i$$

$$\text{Ei} = E(\eta_i)$$

$$\{\sigma_i\} = [E_i]\{\varepsilon_i\}$$

U_c: the energy of structural compliance, η_i: the internal pseudo-densities that are assigned to each element (i) in the topology problem, V: the computed volume, V_o: the original volume, V^*: the amount of material to be removed, V_i: the volume of element (i), E_i: the elasticity tensor for each element, E: the elasticity tensor, σ_i: the stress vector of element (i), ε_i: the strain vector of element (i).

The density variable, η, varied between 0 and 1, where an η_i closer to 0 represented material to be retained and an η_i closer to 1 represented material that should be removed. The topological optimization of the structural simulation was performed for flexion, extension, lateral bending, and torsion. To determine whether enough material was removed by topology optimization, the study set an excessive volume reduction, as determined by a 50 % volume reduction and 20 iterations. The convergence tolerance was defined as 0.0001. Then, the final design of this new rod, termed the topology-I rod (Fig. 2), was obtained from the topology optimization. The volume of the topology-I rod was reduced by approximately 39 % compared to that of a rigid rod ($\Phi 6 \times$ L46). The location of the effective material from the topology optimization was in anterior–posterior (AP) direction of the rod. Therefore, we removed some material from the medial–lateral direction of the rod, and it was shaped like an I-rod.

Additionally, we created a sleeve mechanism in between the caudal screw (screw hole $\Phi 7$ mm) and rod ($\Phi 6$ mm) in the TD model (Fig. 3). We expected that the TD system would not be rigid in extension and lateral bending because the facet joints can support some forces. Therefore, we added a sleeve to the distal end of the rod to allow for relative movement to reduce the rigidity of the spinal implant in extension and lateral bending. Hence, we expected the TD model to induce less stiffness because of topology optimization and its mobility.

2.3 FE model of the DY and TD systems

The DY [27, 30] and TD models (Fig. 3) were bilaterally inserted into the L3–L4 level of the FE model. The implant for the DY model consisted of four titanium alloy screws (Diameter: 6.4 mm, Length: 45 mm, Hole diameter: 6 mm). Moreover, we modelled two PCU spacers (Diameter: 12 mm, Length: 30 mm) and two PET cords that contacted the screw in the DY model. In the TD FE model, the implant consisted of four titanium alloy screws (Diameter: 6.4 mm, Length: 45 mm, Hole diameter: 6 and 7 mm) and two titanium alloy topology-I rods ($\Phi 6 \times \Phi 8 \times$ L48 mm). The topology-I rods were bound to the L3 screws and contacted the L4 screws. Therefore, the TD system was mobile between the lower pedicle

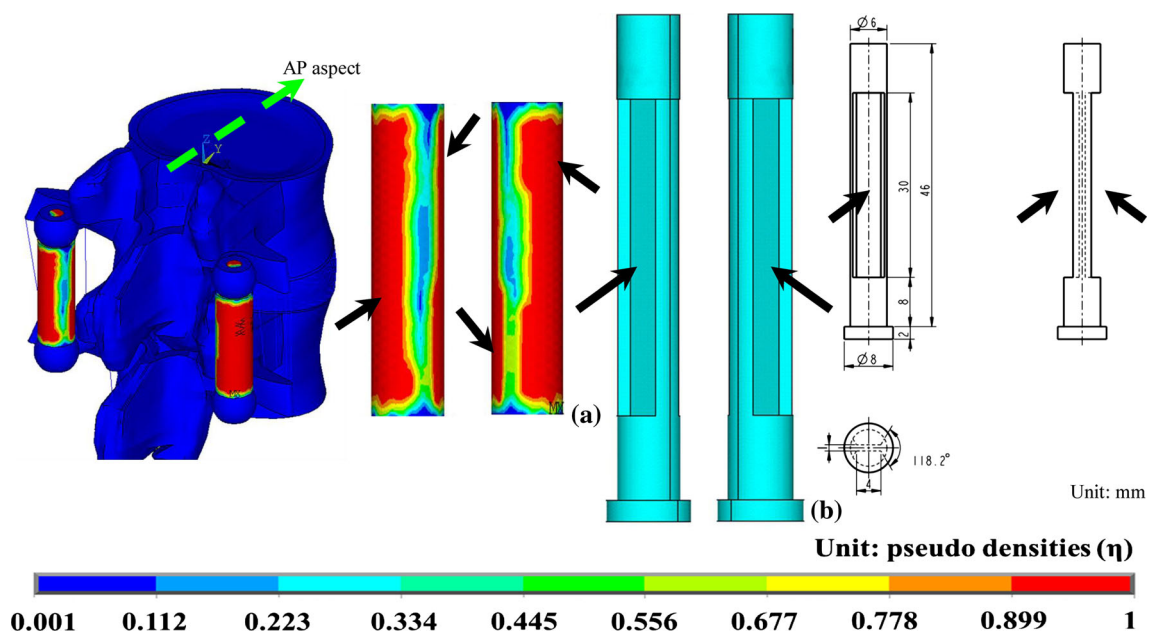| 0.001 | 0.112 | 0.223 | 0.334 | 0.445 | 0.556 | 0.677 | 0.778 | 0.899 | 1 |

Unit: pseudo densities (η)

Fig. 2 Results of topology optimization: **a** The rigid rod in the L3–L4 motion segment, the *arrow* indicates the location of redundant material in anterior–posterior (AP) aspect of spinal model; **b** the new design (topology-I rod); **c** the size of the topology-I rod
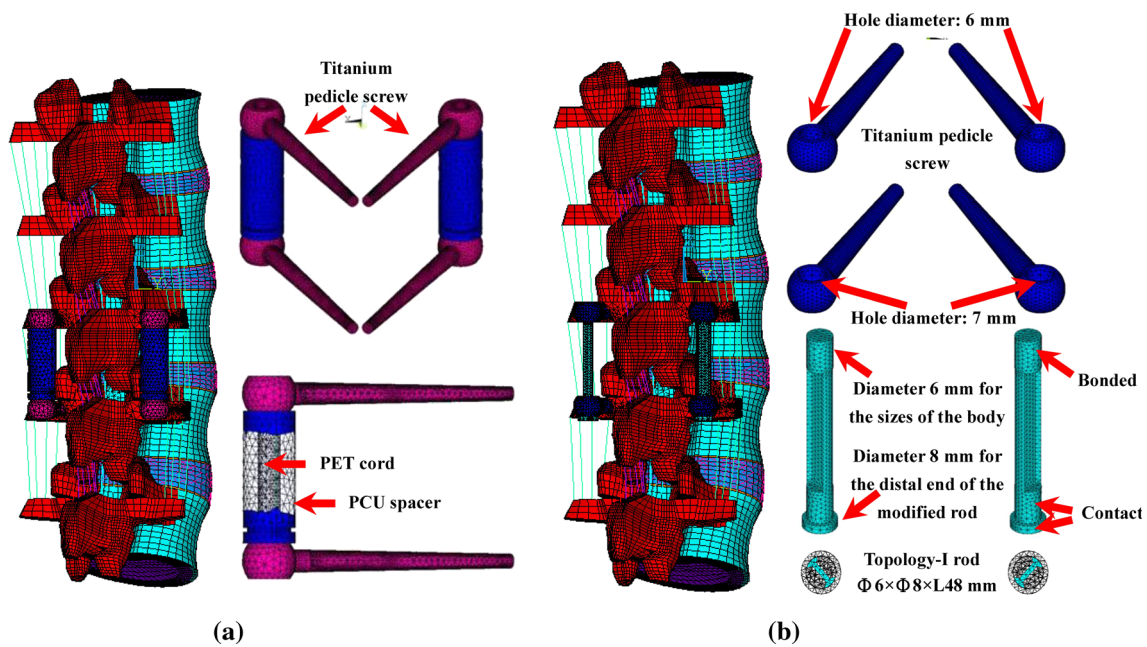
Fig. 3 FE model: **a** DY system and **b** TD system

screw and the rod in extension (rod: Φ6 × Φ8 mm plus screw hole diameter: Φ7 mm), which could support similar normal stiffness. Previous reports [35–37] have indicated that a mobile implant could restore the ROM and stiffness to a normal behaviour. The DY model consisted of 292,502 elements and 126,090 nodes. The TD model included 224,960 elements and 116,751 nodes. The material properties of the implant were based on information from previous studies [27, 30, 38].

2.4 Boundary and loading conditions

Several studies indicated that controlling the ROM is a reasonable approach for predicting the effects of implanted spinal instrumentation on adjacent levels [29, 39, 40]. This study implemented a hybrid-controlled [29, 39, 40] analysis. A preload of 150 N was applied to the superior surface of the L1 level, as described in the in vitro study by Yamamoto et al. [41]. In addition, the PET cord pretension of 300 N in the DY model was simulated in a link element produced by initial strain [27, 30]. A moment was applied to the top surface of the L1 vertebral body. All nodes pertaining to the bottom surface of the L5 vertebral body were fixed. The ROMs under flexion, extension, torsion, and lateral bending were set at 12°, 10°, 8°, and 20°, respectively. These load values were copied from previous studies [27, 30], which corresponded to 9.97, 12.47, 26.57, and 12.13 Nm, respectively, in the DDD model (Table 1).

3 Results

We compared the biomechanical behaviour of the lumbar spine using the DY and TD models.

3.1 ROM of the lumbar spine

The TD and DY models reduced the ROMs at the bridged level. The ROMs from the bridged level for all motions of the TD and DY models were, at most, 0.94 and 0.88 times those of the DDD model (Table 1). In flexion, the ROM of the TD model was greater than that of the DY model. The stiffness of the TD model was, at most, 1.19 times the stiffness of the DDD model in extension, lateral bending, and torsion. Additionally, the stiffness of the DY model was, at most, 1.15 times the stiffness of the DDD model in extension, lateral bending, and torsion.

3.2 Stress on the adjacent disc

The cranial adjacent disc stresses (CADS) of the TD and DY models were 1.22 and 1.35 times the L2–L3 disc stress of the DDD model (Table 2) in flexion. However, the CADS in the TD model were similar to those in the DY model in extension, lateral bending, and torsion. The CADS values only were varied by 7 % between these models.

Additionally, the TD model decreased the high stress region in the CADS in flexion relative to the same region in

Table 1 ROM comparison for each motion segment in the three FE models

Motion	Model	L1–L2 (degree)	L2–L3 (degree)	L3–L4 (degree)	L4–L5 (degree)	Moment (Nm)	L1–L5 stiffness (Nm/degree)
Flexion	DDD	2.54	2.82 (100 %)	2.94 (100 %)	3.75	9.97	0.83 (100 %)
	DY	3.42	3.63 (129 %)	0.06 (2 %)	4.87	14.60	1.22 (147 %)
	TD	3.14	3.32 (118 %)	0.87 (30 %)	4.49	13.18	1.11 (133 %)
Extension	DDD	2.30	2.35 (100 %)	2.27 (100 %)	3.14	12.47	1.24 (100 %)
	DY	2.36	2.39 (102 %)	1.90 (84 %)	3.32	13.18	1.32 (107 %)
	TD	2.34	2.39 (102 %)	2.13 (94 %)	2.99	9.86	1.30 (105 %)
Lateral bending	DDD	4.11	4.60 (100 %)	5.05 (100 %)	6.14	26.57	1.33 (100 %)
	DY	4.69	5.23 (114 %)	3.05 (60 %)	6.98	30.17	1.51 (114 %)
	TD	4.50	4.99 (108 %)	3.85 (76 %)	6.66	29.46	1.47 (111 %)
Torsion	DDD	1.60	1.75 (100 %)	2.07 (100 %)	2.35	12.13	1.56 (100 %)
	DY	1.72	1.84 (105 %)	1.83 (88 %)	2.55	14.20	1.79 (115 %)
	TD	1.78	1.81 (103 %)	1.64 (79 %)	2.54	14.44	1.86 (119 %)

The parentheses indicate the following value: $\frac{\text{DDD, DY, or TD}}{\text{DDD}} \times 100\%$

the DY model (Fig. 4a). Moreover, the stress distribution of the TD model was similar to that of the DY model in extension, lateral bending, and torsion (Fig. 4b, d).

3.3 Facet contact forces (FCF)

The TD model decreased the L2–L3 and the L3–L4 FCF compared to the DY model in lateral bending and torsion. However, the TD model was similar to the DY model in the L2–L3 FCF, and it increased the L3–L4 FCF compared with the corresponding values in the DY model in extension. The L2–L3 FCF of the TD model was, at most, 1.07 times that of the DDD model and 1.06 times the L3–L4 FCF of the DDD model (Table 3).

3.4 Stress on the pedicle screw

In flexion, extension, and lateral bending, the pedicle screw of the TD model exhibited less stress than it did in the DY model (Fig. 5). The maximum screw stress of the TD model was 0.7 times that of the DY model. However, the minimum stress in extension for the TD model was 0.23 times that of the DY model. Regarding torsion, the TD model demonstrated greater screw stress than the DY model. The maximum screw stress of the TD model was 2.46 times that of the DY model in the L3 screw in torsion. However, in the L4 screw, a similar stress distribution trend was observed between the TD and DY models in torsion. As for the rod stress, the maximum stresses were 60 MPa under flexion, 190 kPa under extension, 292 MPa under lateral bending, and 272 MPa under torsion.

4 Discussion

In this study, the model was validated to compare ROM and disc stress distribution. The validation results were consistent with those of previous in vitro studies [32]. The biomechanical behaviour of the lumbar spine with DY was also compared to other studies. This FE analysis showed that the insertion of DY reduced the ROM of the implanted level in flexion and lateral bending, and less so in extension. Our results agree with a majority of the previous biomechanical studies, as the DY reduced the ROM below the magnitude of the intact spine for the implanted level under flexion and lateral bending [9, 14, 15, 17]. Kiapour et al. [42] predicted that the upper adjacent level slightly increased the ROM (extension: 4 %; torsion: 4 %), and a similar trend was observed in our FE study (extension: 2 %; torsion: 5 %). Some clinical studies have reported signs of degeneration adjacent to the surgical level in between 9.6 and 29 % [8, 43] of cases using the DY system. From their clinical observation, the previous researchers presumed that the DY system acts as a rigid fixator. This FE study found a remarkable increase in the annulus stress at the adjacent levels when using DY, and this result was consistent with those of an earlier in vitro study [18]. Therefore, DY is likely to increase the annulus stress at the adjacent levels and cannot restore normal load sharing to the lumbar spine; however, the stress-shielding effect on adjacent levels was still less than that of a rigid fixator [9].

The TD system was expected to be a dynamic stabilization system. The basic intent of a dynamic stabilization system is to reduce the stiffness of the rigid fixation system

to allow limited motion at the implanted level while preventing the concentration of stress at adjacent levels. The primary finding of our study demonstrated that the TD

Table 2 Comparison of disc stresses in the three FE models

Motion	Model	L2–L3	L3–L4
Unit: kPa			
Flexion	DDD	792 (100 %)	737 (100 %)
	DY	1,070 (135 %)	282 (38 %)
	TD	965 (122 %)	302 (41 %)
Extension	DDD	689 (100 %)	645 (100 %)
	DY	700 (102 %)	492 (76 %)
	TD	701 (102 %)	585 (91 %)
Lateral bending	DDD	1,590 (100 %)	1,570 (100 %)
	DY	1,910 (120 %)	1,060 (68 %)
	TD	1,800 (113 %)	1,420 (90 %)
Torsion	DDD	386 (100 %)	407 (100 %)
	DY	451 (117 %)	559 (137 %)
	TD	434 (112 %)	315 (77 %)

The parentheses indicate the following value: $\frac{\text{DDD, DY, or TD}}{\text{DDD}} \times 100\%$

system exhibited the traits of a dynamic stabilization system, similar to the DY system. However, the TD system exhibited lower stiffness in flexion than the DY system because the DY system had greater cord pretension, thus allowing it to resist the flexion moment. Additionally, the TD system containing a sleeve mechanism also offered improved mobility. Therefore, we found that the increase in adjacent disc stress in the TD system was lower than that of the DY system.

When a stiff system is implanted, the screw pedicle screw can loosen, and implant failure is more likely to occur in the long term [37]. Similarly, the dynamic stabilization system was developed as a soft-stiffness system; screw loosening and implant failure are rare relative to the rigid fixation system. A previous clinical study [10] reported screw loosening (3 of 26 patients) and screw breakage (one patient) in the DY system at a 4-year follow-up. The TD system containing a sleeve mechanism allows for limited motion, and force is transmitted to the facet joint. Therefore, the screw stresses from the TD system were much smaller than those generated in the DY system in flexion, extension, and lateral bending. The reduction in
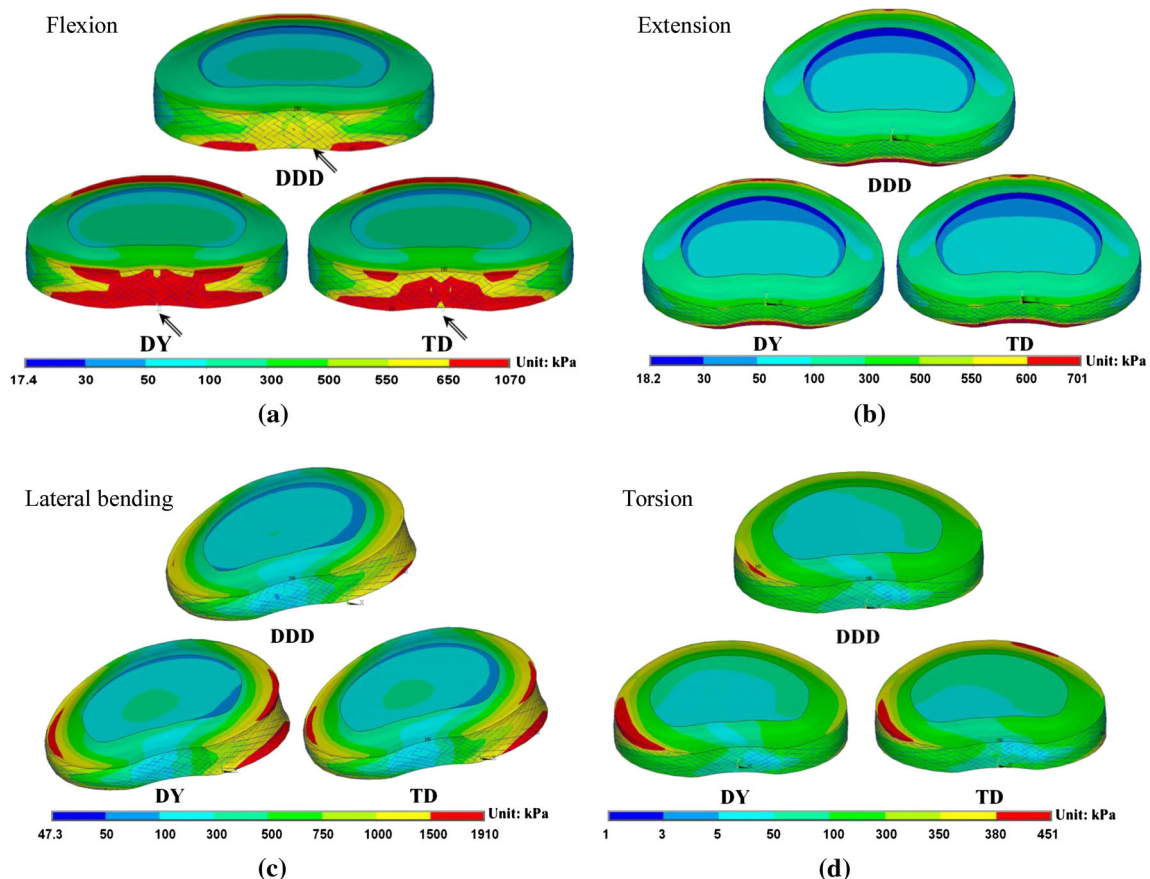

Fig. 4 A von-Mises stress distribution was observed for the cranial adjacent disc in L2–L3 for all motions. The *arrowhead* indicates the range of higher stress distribution

Table 3 Comparison of facet joint forces in the three FE models

Motion	Model	L2–L3	L3–L4
Unit: N			
Extension	DDD	44 (100 %)	87 (100 %)
	DY	47 (107 %)	46 (53 %)
	TD	47 (107 %)	78 (90 %)
Lateral bending	DDD	27 (100 %)	31 (100 %)
	DY	29 (107 %)	45 (145 %)
	TD	21 (78 %)	33 (106 %)
Torsion	DDD	147 (100 %)	141 (100 %)
	DY	167 (114 %)	164 (116 %)
	TD	41 (28 %)	63 (45 %)

The parentheses indicate the following value: $\frac{\text{DDD, DY, or TD}}{\text{DDD}} \times 100\,\%$

pedicle screw stresses may prolong the life of pedicle screw in fatigue performance. However, in torsion, the TD system exhibited greater screw stress than did the DY system, as the stiffness of the bridged level (8.8 Nm/degree) from the TD system was greater than that of the bridged level (7.8 Nm/degree) from the DY system. Therefore, the stress-shielding effect on the implant from the TD system is greater than that of the DY system in torsion.

In terms of FCF, the greatest change in the DY system occurred in extension rather than torsion; this finding was consistent with an earlier FE study [9]. However, the FCF from the TD system only changed slightly in extension. The TD system was similar to the intact spine for the FCF because of the mobility in sleeve mechanism. This result

indicates that greater force is transmitted via the facet joint form L3 to L4 in the TD system due to the facet arthroplasty system. However, in torsion, the TD system had lower FCF at the adjacent level. This finding may be attributed to the fact that the sleeve did not offer a sliding effect on the transverse plane. As a result, the screw and rod could resist most twisting torque, so less force was transmitted to the facet joint. Based on our results, we believe that the sliding feature influences the facet loads at the bridged level and the adjacent level.

The limitations of the FE analysis are as follows: (1) the material properties, including the bilinear behaviour of the spinal ligaments and the degeneration of the disc, were simplified and idealized from those of a cadaveric specimen. The past study [44] demonstrated that the linear behaviour of the ligaments only had a minor effect on the ROM as compared with the nonlinear behaviour of the ligaments. Also, the spinal ligament force was much lower than the vertebral body force as well. Therefore, this study only considered the linear behaviour to simulate the spinal ligament. (2) The lordosis angle and characteristics of disc degeneration, such as dehydration and reduced disc height, were not considered; a previous study reported that disc degeneration would decrease intradiscal pressure and ROM [45]. Because disc degeneration stiffens the lumbar spine, this study only modified the Young's modulus of the intervertebral disc to compare with in vitro tests to confirm the reality of the lumbar spine model. Our FE analysis was in agreement with the previous in vitro test. (3) The thread on the pedicle screw was ignored. Because we wanted to
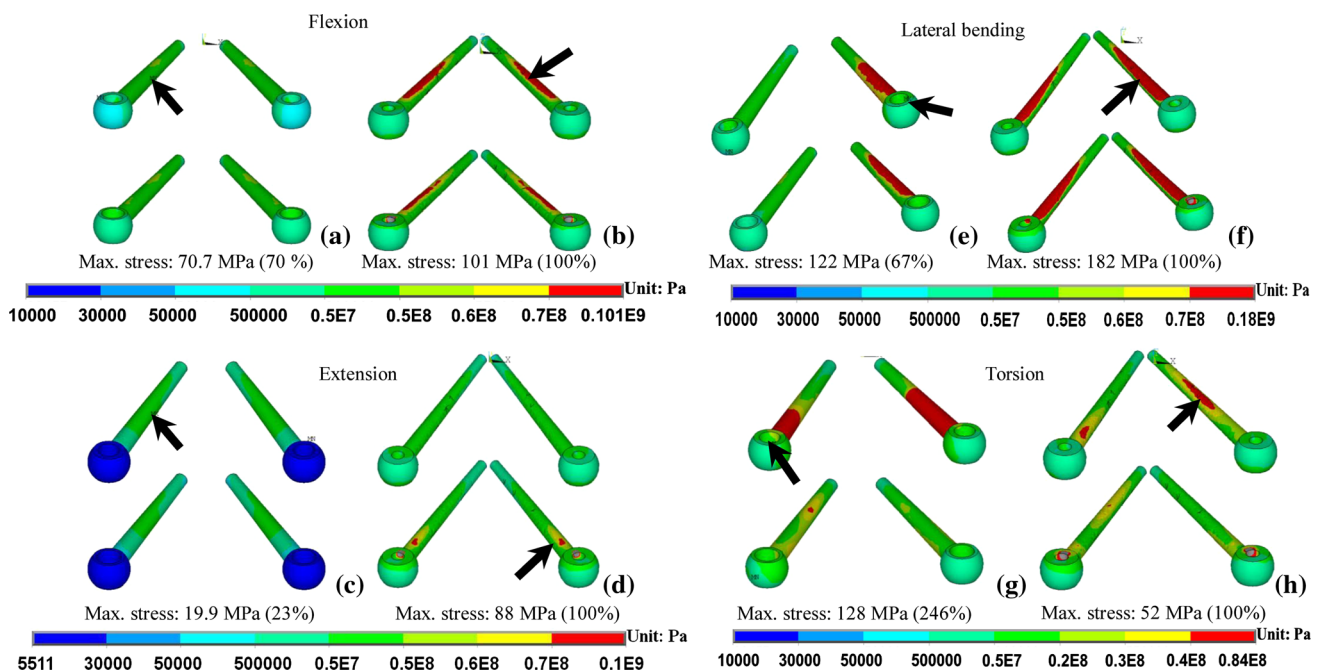

Fig. 5 Screw stress distribution for all motions. The *arrowhead* indicates the position of maximum stress (Right: DY system, Left: TD system)

507

investigate how the new design affects spinal biomechanics rather than the mechanical interaction between screw thread and bone, we assumed complete osseointegration between the bone and screw after a period of time. Without the screw thread, the stress analysis of the pedicle screw was likely underestimated. Thus, the conclusions of this study were made under the above limitations. (4) If the lordotic curve or fixation level of lumbar spine was changed in the topology optimization analysis, the modification of dynamic spinal fixator was possible to give a sight alteration. (5) This study only predicted the load distribution using FE method, but this study did not know the real situation of wear debris in between sleeve and the distal end of the rod. Wear experiments are suggested to be conducted in the future.

5 Conclusion

Topology optimization indicated that the effective region of the rod was located in the AP direction and reshaped as an I-beam rod. The new TD system with the modified rod achieved less stiffness and was comparable to the DY system; however, the increase in adjacent disc stress was alleviated, which could avoid early disc degeneration. However, in torsion, the pedicle screw stress increased, and the facet joint contact force decreased.

References

1. Erbulut DU, Zafarparandeh I, Ozer AF, Goel VK (2013) Biomechanics of posterior dynamic stabilization systems. Adv Orthop 2013:451956. doi:10.1155/2013/451956
2. Anand N, Baron E (2013) Minimally invasive approaches for the correction of adult spinal deformity. Eur Spine J 22(Suppl 2):S232–S241
3. Fritzel P, Hagg O, Wessberg P, Nordwall A, Swedish Lumbar Spine Study Group (2001) 2001 volvo award winner in clinical studies: lumbar fusion versus nonsurgical treatment for chronic low back pain. Spine 26(23):2521–2534
4. Gibson JN, Grant IC, Waddell G (1999) The Cochrane review of surgery for lumbar disc prolapse and degenerative lumbar spondylosis. Spine 24(17):1820–1832
5. Eck JC, Humphreys SC, Hodges SD (1999) Adjacent-segment degeneration after lumbar fusion: a review of clinical, biomechanical, and radiologic studies. Am J Orthop 28(6):336–340
6. Schlegel JD, Smith JA, Schleusener RL (1996) Lumbar motion segment pathology adjacent to thoracolumbar, lumbar, and lumbosacral fusions. Spine 21(8):970–981
7. Gardner A, Pande KC (2002) Graf ligamentoplasty: a 7-year follow-up. Eur Spine J 11(Suppl 2):S157–S163
8. Stoll TM, Dubois G, Schwarzenbach O (2002) The dynamic neutralization system for the spine: a multi-center study of a novel non-fusion system. Eur Spine J 11(Suppl 2):S170–S178
9. Rohlmann A, Burra NK, Zander T, Bergmann G (2007) Comparison of the effects of bilateral posterior dynamic and rigid fixation devices on the loads in the lumbar spine: a finite element analysis. Eur Spine J 16(8):1223–1231
10. Schaeren S, Broger I, Jeanneret B (2008) Minimum four-year follow-up of spinal stenosis with degenerative spondylolisthesis treated with decompression and dynamic stabilization. Spine 33(18):636–642
11. Würgler-Hauri CC, Kalbarczyk A, Wiesli M, Landolt H, Fandino J (2008) Dynamic neutralization of the lumbar spine after microsurgical decompression in acquired lumbar spinal stenosis and segmental instability. Spine 33(3):66–72
12. Kim CH, Chung CK, Jahng TA (2011) Comparisons of outcomes after single or multilevel dynamic stabilization: effects on adjacent segment. J Spinal Disord Tech 24(1):60–67
13. Eberlein R, Holzapfel A, Frohlich M (2004) Multi-segment FEA of the human lumbar spine including the heterogeneity of the annulus fibrosus. Comput Mech 34(2):147–163
14. Freudiger S, Dubios G, Lorrain M (1999) Dynamic neutralization of the lumbar spine confirmed on a new lumbar spine simulator in vitro. Arch Orthop Trauma Surg 119(3–4):127–132
15. Niosi CA, Zhu QA, Wilson DC, Keynan O, Wilson DR, Oxland TR (2006) Biomechanical characterization of the three-dimensional kinematic behavior of the Dynesys dynamic stabilization system: an in vitro study. Eur Spine J 15(6):913–922
16. Zander T, Rohlmann A, Burra NK, Bergmann G (2006) Effect of a posterior dynamic implant adjacent to a rigid spinal fixator. Clin Biomech (Bristol, Avon) 21(8):767–774
17. Schmoelz W, Huber JF, Nydegger T, Dipl-Ing, Claes L, Wilke HJ (2003) Dynamic stabilization of the lumbar spine and its effects on adjacent segments: an in vitro experiment. J Spinal Disord Tech 16(4):418–423
18. Schmoelz W, Huber JF, Nydegger T, Claes L, Wilke HJ (2006) Influence of a dynamic stabilization system on load bearing of a bridged disc: an in vitro study of intradiscal pressure. Eur Spine J 15(8):1276–1285
19. Niosi CA, Wilson DC, Zhu Q, Keynan O, Wilson DR, Oxland TR (2008) The effect of dynamic posterior stabilization on facet joint contact forces. Spine 33(1):19–26
20. Zhong ZC, Wei SH, Wang JP, Feng CK, Chen CS, Yu CH (2006) Finite element analysis of the lumbar spine with a new cage using a topology optimization method. Med Eng Phys 28(1):90–98
21. Lin CY, Wirtz T, LaMarca F, Hollister SJ (2007) Structural and mechanical evaluations of a topology optimized titanium interbody fusion cage fabricated by selective laser melting process. J Biomed Mater Res A 83(2):272–279
22. Bendsoe MP, Kikuchi N (1988) Generating optimal topologies in structural design using a homogenization method. Comput Methods Appl Mech Eng 71(2):197–224
23. Suzuki K, Kikuchi N (1991) A homogenization method for shape and topology optimization. Comput Methods Appl Mech Eng 93(3):291–318
24. Chang CL, Chen CS, Huang CH, Hsu ML (2012) Finite element analysis of the dental implant using a topology optimization method. Med Eng Phys 34(7):999–1008
25. Liao YC, Feng CK, Tsai MW, Chen CS, Cheng CK, Ou YC (2007) Shape modification of the Boston brace using a finite element method with topology optimization. Spine 32(26):3014–3019
26. Huang SY, Lin YH, Liu CL, Wei SH, Feng CK, Chen CS (2007) Rubber band selection for a dynamic splint for flexor tendon repair-A finite element study. J Med Biol Eng 27(3):156–160
27. Liu CL, Zhong ZC, Hsu HW, Shih SL, Wang ST, Hung C, Chen CS (2011) Effect of the cord pretension of the Dynesys dynamic stabilization system on the biomechanics of the lumbar spine: a finite element analysis. Eur Spine J 20(11):1850–1858

28. Chen SH, Zhong ZC, Chen CS, Chen WJ, Hung C (2009) Biomechanical comparison between lumbar disc arthroplasty and fusion. Med Eng Phys 31(2):244–253

29. Zhong ZC, Chen SH, Hung CH (2009) Load- and displacement controlled finite element analyses on fusion and non-fusion spinal implants. Proc Inst Mech Eng H 223(2):143–157

30. Liu CL, Zhong ZC, Shih SL, Hung C, Lee YE, Chen CS (2010) Influence of Dynesys system screw profile on adjacent segment and screw. J Spinal Disord Tech 23(6):410–417

31. Umehara S, Tadano S, Abumi K, Katagiri K, Kaneda K, Ukai T (1996) Effects of degeneration on the elastic modulus distribution in the lumbar intervertebral disc. Spine 21(7):811–819

32. Kettler A, Rohlmann F, Ring C, Mack C, Wilke HJ (2011) Do early stages of lumbar intervertebral disc degeneration really cause instability? Evaluation of an in vitro database. Eur Spine J 20(4):578–584

33. Wilke HJ, Rohlmann F, Neidlinger-Wilke C, Werner K, Claes L, Kettler A (2006) Validity and interobserver agreement of a new radiographic grading system for intervertebral disc degeneration: part I. Lumbar spine. Eur Spine J 15(6):720–730

34. Galbusera F, Bellini CM, Anasetti F, Ciavarro C, Lovi A, Brayda-Bruno M (2011) Rigid and flexible spinal stabilization devices: a biomechanical comparison. Med Eng Phys 33(4):490–496

35. Zhu Q, Larson CR, Sjovold SG, Rosler DM, Keynan O, Wilson DR, Cripton PA, Oxland TR (2007) Biomechanical evaluation of the total facet arthroplasty system: 3-dimensional kinematics. Spine 32(1):55–62

36. Phillips FM, Tzermiadianos MN, Voronov LI, Havey RM, Carandang G, Renner SM, Rosler DM, Ochoa JA, Patwardhan AG (2009) Effect of the total facet arthroplasty system after complete laminectomy-facetectomy on the biomechanics of implanted and adjacent segments. Spine J 9(1):96–102

37. Goel VK, Mehta A, Jangra J, Faizan A, Kiapour A, Hoy RW, Fauth AR (2007) Anatomic facet replacement system (AFRS) restoration of lumbar segment mechanics to intact: a finite element study and in vitro cadaveric investigation. SAS J 1(1):46–54

38. Chiang MF, Teng JM, Huang CH, Cheng CK, Chen CS, Chang TK, Chao SH (2004) Finite element analysis of cage subsidence in cervical interbody fusion. J Med Biol Eng 24(4):201–208

39. Goel VK, Grauer JN, Patel TCh, Biyani A, Sairyo K, Vishnubhotla S, Matyas A, Cowgill I, Shaw M, Long R, Dick D, Panjabi MM, Serhan H (2005) Effects of charité artificial disc on the implanted and adjacent spinal segments mechanics using a hybrid testing protocol. Spine 30(24):2755–2764

40. Panjabi M, Henderson G, Abjornson C, Yue J (2007) Multidirectional testing of one- and two-level ProDisc-L versus simulated fusions. Spine 32(12):1311–1319

41. Yamamoto I, Panjabi MM, Crisco T, Oxland T (1989) Three-dimension movement of the whole lumbar spine and lumbosacral joint. Spine 14(11):1256–1260

42. Kiapour A, Ambati D, Hoy RW, Goel VK (2012) Effect of graded facetectomy on biomechanics of Dynesys dynamic stabilization system. Spine 37(10):E581–E589

43. Vaga S, Brayda-Bruno M, Perona F, Fornari M, Raimondi MT, Petruzzi M, Grava G, Costa F, Caiani EG, Lamartina C (2009) Molecular MR imaging for the evaluation of the effect of dynamic stabilization on lumbar intervertebral discs. Eur Spine J 18(Suppl 1):40–48

44. Kim H, Lim DH, Oh HJ, Lee KY, Lee SJ (2011) Effects of nonlinearity in the materials used for the semi-rigid pedicle screw systems on biomechanical behaviors of the lumbar spine after surgery. Biomed Mater 6(5):055005

45. Park WM, Kim K, Kim YH (2013) Effects of degenerated intervertebral discs on intersegmental rotations, intradiscal pressures, and facet joint forces of the whole lumbar spine. Comput Biol Med 43(9):1234–1240